

The submitted manuscript has been authored by a contractor of the U. S. Government under contract No. W-31-109-ENG-38. Accordingly, the U. S. Government retains a nonexclusive, royalty-free license to publish or reproduce the published form of this contribution, or allow others to do so, for U. S. Government purposes.

A RELATIVISTIC DESCRIPTION OF DEFORMED NUCLEI*

Charles E. Price
Physics Division
Argonne National Laboratory
Argonne, IL 60439

CONF-880386--6
DE88 012033

INTRODUCTION

In recent years relativistic mean field calculations have successfully reproduced the properties of spherical nuclei using parameters that are fit to the empirical binding energy and saturation density of nuclear matter.¹ Specifically, the large scalar and vector mean fields that are a characteristic of this model lead to a natural inclusion of the large spin-orbit splittings that are present in real nuclei. Unfortunately, the restriction to spherical symmetry effectively limits the model to calculations in five doubly-magic nuclei. In order to extend the model to non-closed shell nuclei it is necessary to include deformations. This makes it possible to determine if the model can provide a good description of deformed nuclei using the same parameters that reproduce the properties of nuclear matter and spherical nuclei.

In contrast to the successful description of spherical nuclei, early calculations for the magnetic moments of closed shell ± 1 nuclei² were in qualitative disagreement with the experimental measurements. In these calculations, the additional particle or hole was treated as a valence particle and was not allowed to effect the closed shell core. This effectively sacrificed the self-consistency of the calculation in favor of simplicity. Subsequent calculations³⁻⁶ have attempted to restore the self consistency by including the effects of the valence particle on the core through a variety of approximations. In general, the results of these calculations are in reasonable agreement with the data and are very similar to the non-relativistic Schmidt moments. In order to carry out a fully self-consistent calculation for these odd-mass nuclei it is again necessary to include deformations.

Another interesting feature of odd-mass nuclei, is that there are additional mean fields that are not present for nuclear matter or for spherical nuclei. These fields are the three vector components of all of the vector fields (ω , ρ and photon fields) and the pion field. So in a very real sense, deformed nuclei provide an area for studying new effects that are not present in calculations for spherical nuclei.

In the following section, we will outline the basic model and describe the calculations for deformed nuclei. Then, in sections 3 and 4, we will present the results of our calculations for axially symmetric nuclei in the s-d shell^{7,8} and for closed shell ± 1 nuclei⁹ respectively. For more detail on the relativistic model see ref. 10 and for the detailed calculations for deformed nuclei refer to refs. 7 - 9.

* Work supported by the U. S. Department of Energy, Nuclear Physics Division, under contract W-31-109-ENG-38.

pp

FORMALISM

The basic starting point for these calculations is a relativistic quantum field theory Lagrangian,

$$\begin{aligned} \mathcal{L} = & \mathcal{L}(\psi, \phi, V, b, \pi, A) \\ & -g_v \bar{\psi} \gamma_\mu \psi V^\mu + g_s \bar{\psi} \psi \phi - \frac{1}{3!} \kappa \phi^3 - \frac{1}{4!} \lambda \phi^4 \\ & -ig_\pi \bar{\psi} \gamma_5 \vec{\tau} \cdot \vec{\pi} \psi - \frac{1}{2} g_\rho \bar{\psi} \gamma_\mu \vec{\tau} \cdot \vec{b}^\mu \psi - e \bar{\psi} \gamma_\mu \frac{1}{2} (1 + \tau_3) \psi A^\mu \end{aligned} \quad (1)$$

which includes the couplings of the nucleons (ψ) to scalar (ϕ), vector (V), rho (b) and pi (π) mesons and the photon (A). It also allows for explicit nonlinear self-couplings of the scalar meson in the form of terms proportional to ϕ^3 and ϕ^4 .

In the Mean-Field or Hartree Approximation, the quantum meson fields are replaced by their expectation values which are classical fields. In this limit, we can write down a simple set of equations of motion for the various fields:

$$[-i\vec{\alpha} \cdot \vec{\nabla} + \gamma_0 \Sigma_H(\vec{x})] U_\alpha(\vec{x}) = \epsilon_\alpha U_\alpha(\vec{x}) \quad (2)$$

where

$$\begin{aligned} \Sigma_H(\vec{x}) = & -g_s \phi(\vec{x}) + g_v \gamma_\mu V^\mu(\vec{x}) + g_\pi \gamma_5 \tau_3 \pi_0(\vec{x}) \\ & + \frac{1}{2} g_\rho \gamma_\mu \tau_3 b_0^\mu(\vec{x}) + e \gamma_\mu \frac{1}{2} (1 + \tau_3) A^\mu(\vec{x}) \end{aligned} \quad (3)$$

and

$$\begin{aligned} (-\vec{\nabla}^2 + m_s^2) \phi(\vec{x}) &= -g_s \text{Tr} [iG_H(\vec{x}, \vec{x})] \\ (-\vec{\nabla}^2 + m_v^2) V^\mu(\vec{x}) &= -g_v \text{Tr} [i\gamma^\mu G_H(\vec{x}, \vec{x})] \\ (-\vec{\nabla}^2 + m_\pi^2) \pi_0(\vec{x}) &= -g_\pi \text{Tr} [i\gamma_5 \tau_3 G_H(\vec{x}, \vec{x})] \\ (-\vec{\nabla}^2 + m_\rho^2) b_0^\mu(\vec{x}) &= -g_\rho \text{Tr} [i\gamma^\mu \tau_3 G_H(\vec{x}, \vec{x})] \\ (-\vec{\nabla}^2) A^\mu(\vec{x}) &= -e \text{Tr} [i\gamma^\mu \frac{1}{2} (1 + \tau_3) G_H(\vec{x}, \vec{x})] \end{aligned} \quad (4)$$

where

$$iG_H(\vec{x}, \vec{x}) = \sum_{\alpha}^{\text{occ}} U_\alpha(\vec{x}) \bar{U}_\alpha(\vec{x}). \quad (5)$$

In eqs. (2) - (5), Σ_H is the Hartree self-energy, G_H is the Hartree Green's function, U_α and ϵ_α are the nucleon orbitals and eigenvalues respectively and α represents a complete set of quantum numbers for the individual orbitals. In the case of deformed nuclei, the total angular momentum is not a good quantum number so α is limited to parity and the third component of the angular momentum, m .

For spherical nuclei, the meson fields are angle independent and the angle dependence of the nucleon orbitals is trivial. In this case, these equations can be rewritten in terms of a set of coupled ordinary differential equations that only depend on the radial coordinate. On the other hand, for deformed nuclei the mean fields have an explicit angle dependence and eqs. (2) - (5) form a set of coupled partial differential equations. In principle, these equations could be solved directly; however, in practice it is much more convenient to use a few simple expansions which make it possible to separate out all of the angular dependence.

Prolate		Oblate	
Level	Energy	Level	Energy
$\frac{1}{2}^+$	-45.6	$\frac{1}{2}^+$	-46.4
$\frac{1}{2}^-$	-28.6	$\frac{3}{2}^-$	-27.0
$\frac{3}{2}^-$	-22.6	$\frac{1}{2}^-$	-25.4
$\frac{1}{2}^-$	-15.6	$\frac{1}{2}^-$	-17.1
$\frac{1}{2}^+$	-12.1	$\frac{1}{2}^+$	-9.4
$E_0 = -103.3 MeV$		$E_0 = -98.5 MeV$	
$Q = 403 mb$		$Q = -199 mb$	

Table 1. Deformed solutions in ^{20}Ne .

For the nucleon orbitals we expand in terms of the usual relativistic spin-angle functions:¹¹

$$U_\alpha(\vec{x}) = \sum_{\kappa} \left[\begin{array}{c} \frac{iG_\alpha^a(r)}{r} \Phi_{\kappa m} \\ -\frac{F_\alpha^a(r)}{r} \Phi_{-\kappa m} \end{array} \right] \quad (6)$$

where the sum over κ effectively mixes components with different total angular momenta but is restricted such that the orbitals have good parity. For the scalar field and the time components of the vector fields we expand in Legendre polynomials:

$$\begin{aligned} \phi(\vec{x}) &= \sum_l \phi_l(r) P_l(\cos \theta) \\ V^0(\vec{x}) &= \sum_l V_l^0(r) P_l(\cos \theta) \end{aligned} \quad (7)$$

where the sum is restricted to even values of l . And finally, the three vector components of the various vector fields are expanded in terms of vector spherical harmonics:¹²

$$\vec{V}(\vec{x}) = i \sum_l V_l(r) \vec{Y}_{ll}^0(\Omega) \quad (8)$$

The resulting angle-independent equations may be solved using standard techniques to obtain the self consistent Hartree ground state. For more detail concerning the solution of these equations see refs. 7, 8 and 9.

RESULTS: EVEN-EVEN NUCLEI

Using the standard Finite Hartree parameters of Horowitz and Serot¹, which have been fitted to the binding energy, saturation density and symmetry energy of nuclear matter, we find both an oblate and a prolate solution for ^{20}Ne . The level energies of the occupied neutron orbitals for each solution are shown in Table 1. As expected for this nucleus, the prolate solution has the lower energy and is therefore the ground state solution. The predicted quadrupole moment of about $400 mb$ is somewhat smaller than the experimental result of roughly $550 mb$. This may indicate that there is a problem with the relativistic model. To test this possibility, we repeated the calculations for

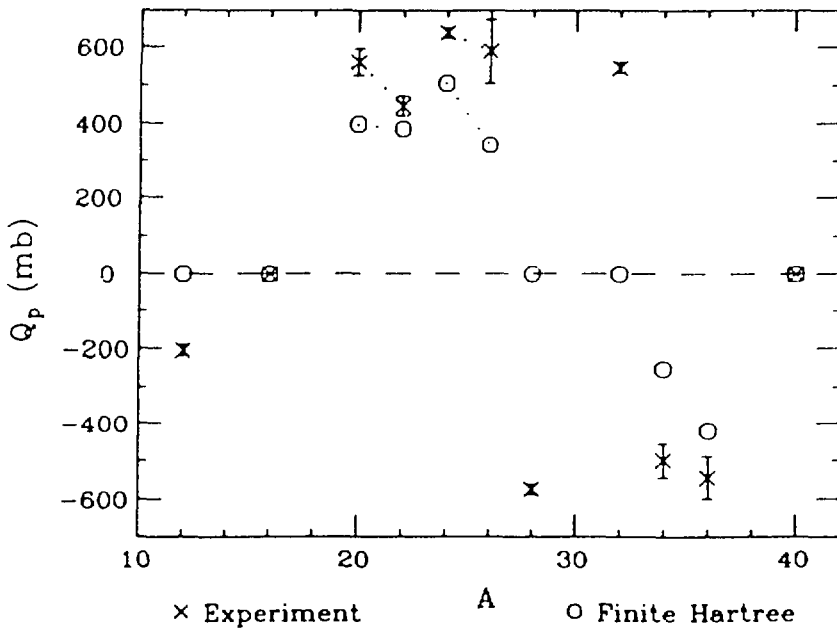


Fig. 1. Quadrupole moments for nuclei in the s-d shell. The crosses with error bars are the experimental results and the circles are the calculated values.

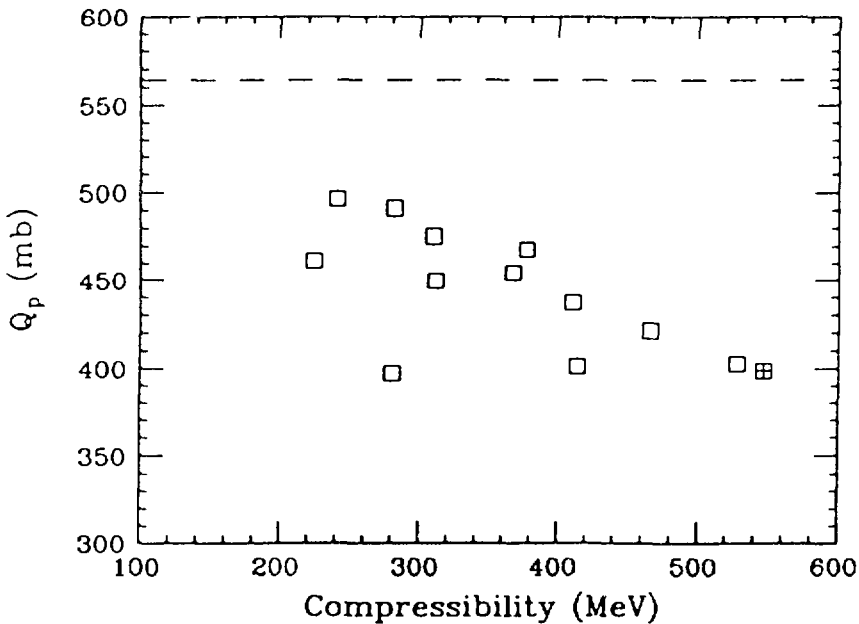


Fig. 2. Compressibility versus quadrupole moment in ^{20}Ne . The dashed line shows the experimental value and the Finite Hartree result is at the extreme right of the figure.

a variety of nuclei throughout the s-d shell. Figure 1 shows the predicted quadrupole moments for these nuclei along with the experimental values.¹³

Clearly, the general trend is that the calculated values are smaller than the experimental results, but more importantly, the relativistic model predicts that all of the closed sub-shell nuclei (e.g. ^{12}C , ^{28}Si , ...) are spherical even though experimentally some of these nuclei are strongly deformed. One possible explanation is that the large value of the compressibility that is a characteristic of this model may be restraining the deformation. A high compressibility indicates that the nucleus is very stiff and has

g_s	g_v	g_p	$m_s^2(\text{MeV})$	$\kappa(\text{MeV})$	λ	M^*/M	$K(\text{MeV})$	$Q_{\text{ch}}(\text{mb})$
109.73	190.59	65.37	520.1	0.	0.	0.54	546.8	399.
108.13	187.15	66.27	519.1	100.	0.	0.55	528.3	403.
101.53	173.73	69.56	514.4	500.	0.	0.58	466.1	421.
84.70	143.00	76.18	497.8	1500.	0.	0.66	367.1	454.
94.01	158.48	73.00	510.0	800.	10.	0.61	420.6	436.
68.32	118.07	80.75	476.7	1500.	50.	0.70	342.9	471.
67.26	118.99	80.59	477.6	500.	100.	0.70	377.3	468.
45.22	80.19	86.65	428.7	2500.	100.	0.78	281.9	491.
27.96	52.44	90.33	368.6	2500.	200.	0.84	240.9	496.
89.95	158.47	73.00	510.0	-1000.	100.	0.61	511.7	429.
52.90	98.65	83.92	455.3	-500.	200.	0.74	378.3	476.
114.93	191.15	65.23	518.9	2000.	-100.	0.54	414.2	401.
95.45	154.93	73.75	505.3	3000.	-100.	0.62	311.4	450.
117.82	188.66	65.88	516.1	4000.	-200.	0.55	280.7	397.
95.11	148.93	74.99	500.8	5000.	-200.	0.63	224.2	461.

Table 2. Relativistic Hartree Parameter Sets.

a large surface energy, so it is reasonable to expect that this would tend to minimize the degree to which nuclei can deform. Unfortunately, in the standard model, the compressibility cannot be varied; however, if we include the allowed nonlinear scalar coupling terms shown in eq. (1), we can find a variety of parameter sets all of which reproduce the properties of infinite nuclear matter and spherical nuclei but which have different compressibilities. The parameter sets that we have used are shown in Table 2. Notice that some of the parameter sets involve negative values for the quartic coupling constant, λ . These parameterizations are not allowed in the strictest sense because the energy is no longer bounded from below; however, if the parameters are treated phenomenologically, the best fit to all the properties of spherical nuclei is obtained with negative values of λ .¹⁴ For this reason we have chosen to include parameter sets with negative λ so that we can fully investigate the sensitivity of the deformations. The next to last column in Table 2 shows the corresponding values of the compressibility of nuclear matter. Clearly, these parameter sets include a wide range of compressibilities.

Figure 2 shows the quadrupole moments predicted using the various parameterizations plotted against the compressibility. Although it is possible to improve the agreement with experiment by including the nonlinear couplings, clearly the compressibility is not strongly correlated with the predicted quadrupole moments. In fact there are four parameter sets with very different compressibilities that all predict quadrupole moments of about 400mb . Apparently, the naive argument that the surface energy (and hence the compressibility) would be the driving force that determined the deformation is incorrect.

The next most obvious possibility is that the strength of the spin-orbit splitting is responsible for controlling the degree of deformation. In non-relativistic calculations it was seen that the spin-orbit force was very important for correctly predicting

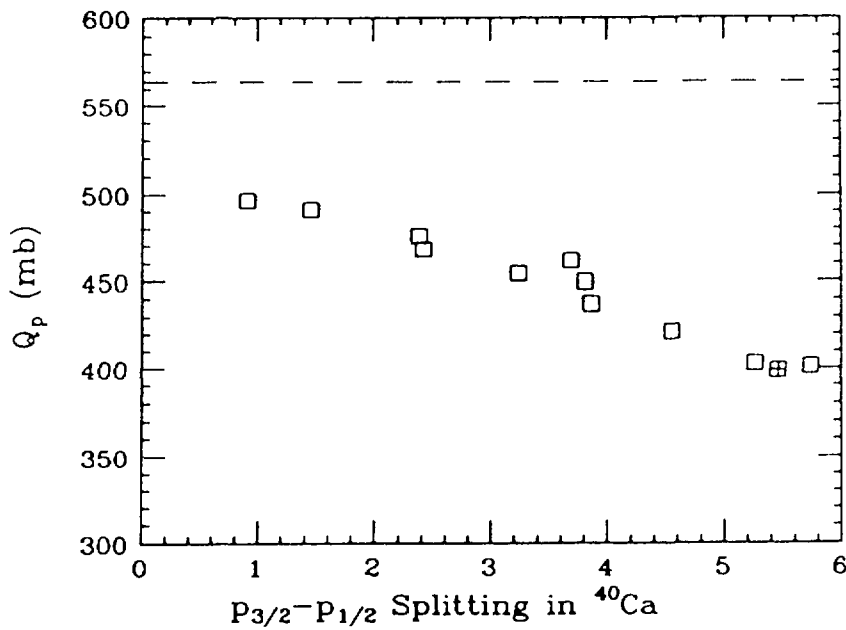


Fig. 3. Spin-orbit splitting in ^{40}Ca versus quadrupole moment in ^{20}Ne . The dashed line shows the experimental value.

Set	g_s	g_v	g_p	m_s^2 (MeV)	κ (MeV)	λ	M^*/M	K (MeV)
A	109.73	190.59	65.37	520.1	0.	0.	0.54	546.8
B	94.01	158.48	73.00	510.0	800.	10.	0.61	420.6
C	95.11	148.93	74.99	500.8	5000.	-200.	0.63	224.2

Table 3. Relativistic Hartree parameter sets.

equilibrium deformations, so it is reasonable to expect that the same will be true for the relativistic calculations. In fact, this is an appealing possibility since the spin-orbit force is automatically included in the relativistic model. Figure 3 shows the quadrupole moments in ^{20}Ne , using the various parameter sets, plotted as a function of the predicted spin-orbit splitting in ^{40}Ca . There is a clear correlation between decreasing spin-orbit splittings and increasing quadrupole moments in this nucleus. In fig. 4, we show the quadrupole moments for nuclei in the s-d shell using three selected parameter sets (see Table 3). Set A is the Finite Hartree linear parameterization, Set C is very similar to the non-linear parameterization of Reinhard *et al.*, and Set B is chosen to give similar agreement with the experimental spin-orbit splitting but with positive quartic coupling. The general agreement with experiment (crosses with error bars) is greatly improved for sets B and C, and more importantly, these sets predict large quadrupole moments for the closed sub-shell nuclei. So throughout the s-d shell, the relativistic model predicts the correct sign and magnitude of the equilibrium deformation provided we use a parameter set which provides a good description of the spin-orbit splitting. Furthermore, fig. 5, which shows a comparison between the results of parameter set B and the results from two non-relativistic calculations using Skyrme interactions,¹⁵ indicates that the relativistic model provides a description of deformed nuclei that is in quantitative agreement with non-relativistic calculations.

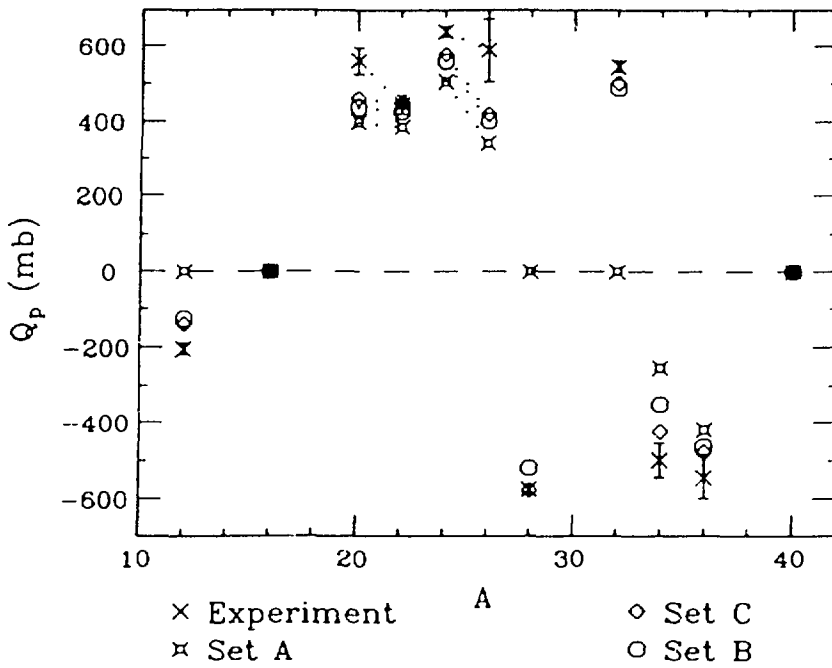


Fig. 4. Quadrupole moments for nuclei in the s-d shell calculated with the parameter sets shown in Table 3.

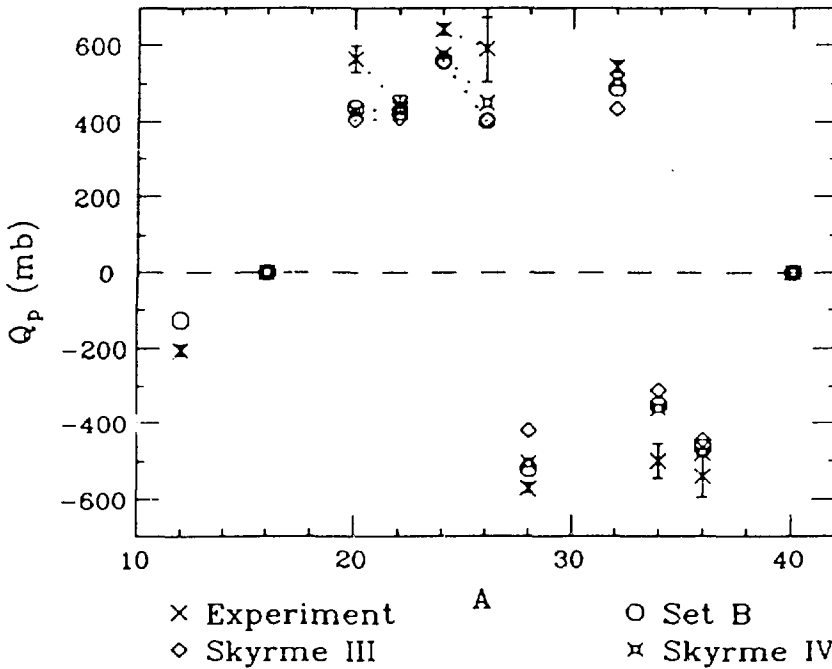


Fig. 5. Comparison of s-d shell quadrupole moments calculated using the relativistic model and non-relativistic Skyrme interactions.

This conclusion is supported by the work of Gambir and Ring.¹⁶ They found that the deformations in the rare earth region can also be correctly predicted in the relativistic model provided that a nonlinear parameterization which gives the correct spin-orbit splitting is used.

RESULTS: CLOSED SHELL ± 1 NUCLEI

In the calculations presented in the preceding section the symmetry of the nuclei limited the mean fields to those that were present for spherical nuclei (*i.e.* the scalar

field and the time components of the vector fields). In this section we consider odd-mass nuclei in which there can be explicit contributions from additional mean fields. Namely, the three vector components of the vector fields and the pion field. Unfortunately, at this time we have no results which include pion effects so the remainder of the discussion will be limited to the inclusion of the three vector fields.

In order to look at the ground state nuclear currents, we must introduce an effective electromagnetic current operator as in refs. 2 and 10. For elastic transitions, the three-vector current operator is

$$\vec{J}(\vec{x}) = \psi^\dagger(\vec{x})Q\vec{\alpha}\psi(\vec{x}) + \frac{1}{2M}\vec{\nabla} \times (\psi^\dagger(\vec{x})\lambda\beta\vec{\Sigma}\psi(\vec{x})) \quad (9)$$

where $\vec{\alpha}$ and β are the usual Dirac matrices and

$$\begin{aligned} Q &\equiv \frac{1}{2}(1 + \tau_3) \\ \lambda &\equiv \lambda_p \frac{1}{2}(1 + \tau_3) + \lambda_n \frac{1}{2}(1 - \tau_3) \\ \vec{\Sigma} &\equiv \begin{pmatrix} \vec{\sigma} & 0 \\ 0 & \vec{\sigma} \end{pmatrix}. \end{aligned} \quad (10)$$

By evaluating this operator in the Hartree ground state, $|J_i\rangle$, the current may be expressed in terms of the nucleon wavefunctions as follows:

$$\langle J_i | \vec{J}(\vec{x}) | J_i \rangle = \sum_{\alpha}^{occ} U_{\alpha}^{\dagger}(\vec{x})Q\vec{\alpha}U_{\alpha}(\vec{x}) + \frac{1}{2M}\vec{\nabla} \times \sum_{\alpha}^{occ} U_{\alpha}^{\dagger}(\vec{x})\lambda\beta\vec{\Sigma}U_{\alpha}(\vec{x}) \quad (11)$$

The first term in eq. (11) is the convection current and is simply the proton contribution to the three-vector source term in eq. (4), and the second term is the anomalous current.

Using these currents, the transverse elastic form factor is given by¹⁷

$$F_T^2(q) = \frac{1}{2J_i + 1} \sum_{J=1,3,\dots}^{2J_i} \left| \langle J_i | \hat{T}_J^{mag}(q) | J_i \rangle \right|^2 \quad (12)$$

where q is the magnitude of the three momentum transfer and

$$\hat{T}_J^{mag}(q) = \int d^3x j_J(qx) \vec{Y}_{JJ_1}^M(\Omega) \cdot \vec{J}(\vec{x}) \quad (13)$$

specifies the transverse magnetic multipoles. In eq. (13), j_J is a spherical Bessel function and $\vec{Y}_{JJ_1}^M$ is a vector spherical harmonic. Finally, the ground state magnetic dipole moment may be obtained from the elastic magnetic form factors as follows:

$$\mu = \lim_{q \rightarrow 0} \left[-i \frac{2M}{q} \left(\frac{6\pi J_i}{(J_i + 1)(2J_i + 1)} \right)^{\frac{1}{2}} \langle J_i | \hat{T}_{J=1}^{mag}(q) | J_i \rangle \right]. \quad (14)$$

In fig. 6, we show the isoscalar contribution to the convection current of eq. (11). The solid curve is the contribution from the valence particle only, which agrees with the early calculations of ref. 2. The dashed curve is taken from ref. 6, in which the effect of the valence particle on the core orbitals is included in the RPA approximation, and the dash-dotted curve is the result calculated from the self-consistent ground

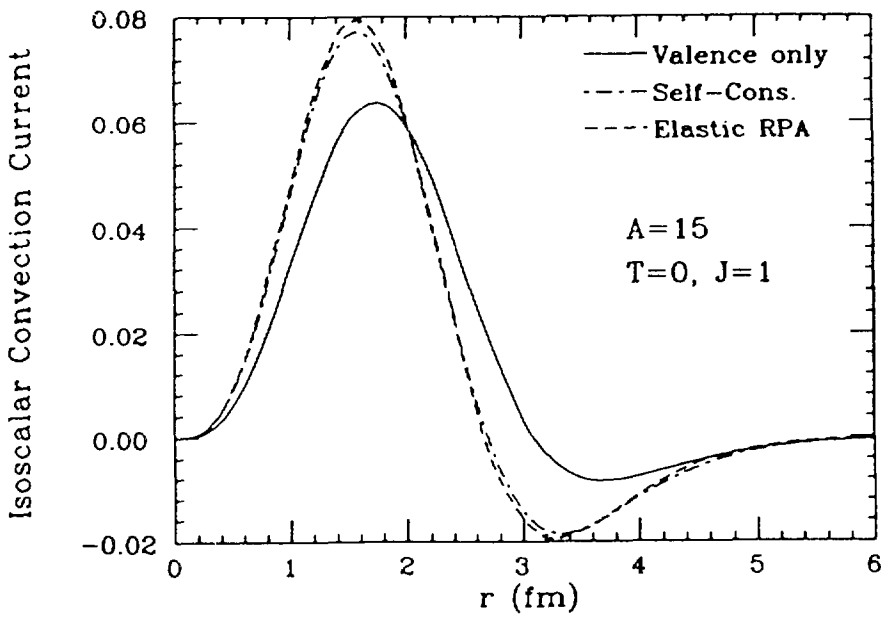


Fig. 6. Isoscalar convection current for the $A = 15$ system. The solid curve is the contribution from the valence orbital, the dashed curve is taken from ref. 6, and the dot-dashed curve is the result obtained from the self-consistent calculations described here.

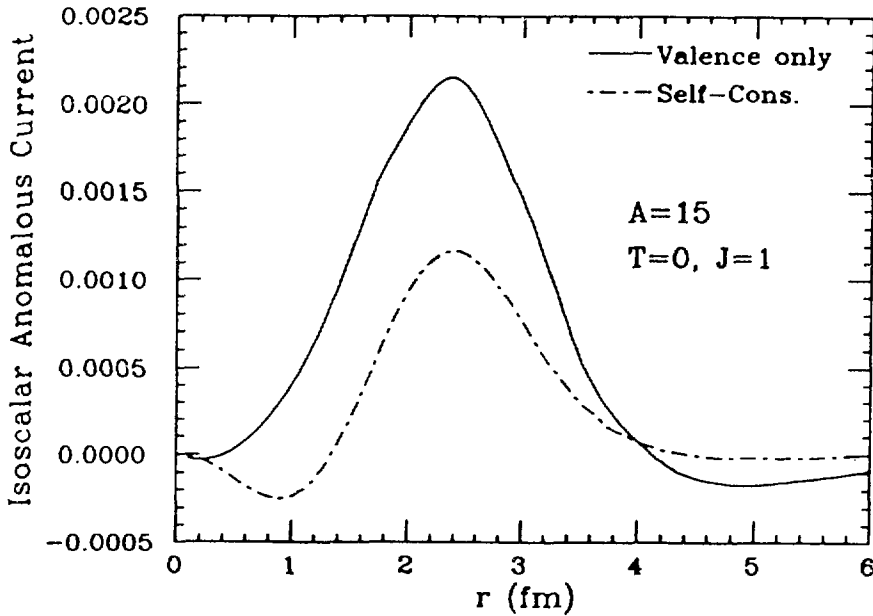


Fig. 7 Isoscalar anomalous current for $A = 15$ as in fig. 6.

state. Clearly the core contribution is significant and cannot be ignored; however, the agreement between the dashed and dash-dotted curves indicates that the RPA is a good approximation for including the core effects in the convection currents. Figure 7 shows the isoscalar contribution to the anomalous current in eq. (11), and again it is clear that the core modifications have a significant effect on the current. Figures 6 and 7 demonstrate the importance of calculating with a self-consistent ground state or at the very least accounting for the self-consistency through an appropriate approximation.

Table 4 shows the magnetic moments for various closed shell ± 1 nuclei. The column

Nucleus	Schmidt	Valence	LDA	Self-Cons.	Expt
^{15}N	-.264	.020	-.149	-.247	-.283
^{15}O	.638	.667	.535	.647	.719
^{17}O	-1.913	-1.905	-2.03	-2.03	-1.894
^{17}F	4.793	5.045	4.901	4.89	4.722
^{39}K	.124	.855	.448	.354	.391
^{39}Ca	1.148	1.170	.848	.968	1.022

Table 4. Magnetic moments on closed shell ± 1 nuclei.

Mass	Orbital	Schmidt	Valence	RPA	Self-Cons.	Expt
15	$1p_{\frac{1}{2}}$.187	.344	.204	.200	.218
17	$1d_{\frac{5}{2}}$	1.44	1.62	1.44	1.43	1.41
39	$1d_{\frac{3}{2}}$.636	1.01	.661	.691	.707

Table 5. Isoscalar magnetic moments.

labeled *Valence* is obtained by including only the contribution of the valence orbital, and the column labeled *LDA* is taken from ref. 5 in which the effects due to the core modifications are included in the local density approximation. Although the valence moments are in clear disagreement with both the experimental values¹⁸ and the non-relativistic Schmidt moments, both the LDA results and the moments obtained from the self-consistent ground states are in good agreement with experiment. This again indicates the importance of including the modifications of the core due to the valence particle. Table 5 shows the corresponding isoscalar moments with the exception that the column labeled *RPA* is obtained from ref. 6.

SUMMARY

In conclusion, we have shown that relativistic Hartree calculations using parameters that have been fit to the properties of nuclear matter can provide a good description of both spherical and axially deformed nuclei. The quantitative agreement with experiment is equivalent to that which was obtained in non-relativistic calculations using Skyrme interactions. We have also shown that the equilibrium deformation is strongly correlated with the size of the spin-orbit splitting, and that parameter sets which give roughly the correct value for this splitting provide the best agreement with the quadrupole moments in the s-d shell. Finally, for closed shell ± 1 nuclei, we showed that the self-consistent calculations are able to reproduce the experimental magnetic moments. This was not possible in relativistic calculations which included only the effects of the valence orbital.

ACKNOWLEDGEMENTS

I am pleased to acknowledge the contributions of my collaborators, G. E. Walker and R. J. Furnstahl.

REFERENCES

1. C. J. Horowitz and B. D. Serot, *Nucl. Phys.* **A368** (1981) 503
2. B. D. Serot, *Phys. Lett.* **107B** (1983) 334
3. J. R. Shepard, E. Rost and C.-Y. Cheung, University of Colorado preprint
4. J. A. McNeil, R. D. Amado, C. J. Horowitz, M. Oka, J. R. Shepard and D. A. Sparrow, *Phys. Rev.* **C34** (1986) 746
5. R. J. Furnstahl and B. D. Serot, *Nucl. Phys.* **A468** (1987) 539
6. R. J. Furnstahl, Indiana University preprint
7. C. E. Price and G. E. Walker, *Phys. Rev.* **C36** (1987) 354
8. R. J. Furnstahl, C. E. Price and G. E. Walker, *Phys. Rev.* **C36** (1987) 2590
9. R. J. Furnstahl and C. E. Price, in preparation
10. B. D. Serot and J. D. Walecka, *Adv. in Nucl. Phys.* **16** (1986) 1
11. J. D. Bjorken and S. D. Drell, *Relativistic Quantum Mechanics*, (McGraw-Hill, New York, 1964)
12. A. R. Edmonds, *Angular Momentum in Quantum Mechanics*, (Princeton University Press, Princeton, 1960)
13. G. Leander and S. E. Larsson, *Nucl. Phys.* **A239** (1975) 93
14. P.-G. Reinhard, M. Rufa, J. Maruhn, W. Greiner and J. Friedrich, *Z. Phys.* **A323** (1986) 13
15. D. Vautherin, *Phys. Rev.* **C7** (1973) 296
16. Y. K. Gambir and P. Ring, *Phys. Lett.* **202B** (1988) 5
17. T. W. Donnelly and J. D. Walecka, *Ann. Rev. of Nucl. Sci.* **25** (1975) 329
18. C. Lederer, J. M. Hollander and I. Perlman, *Table of Isotopes* (J. Wiley and Sons, New York, 1967)

DISCLAIMER

This report was prepared as an account of work sponsored by an agency of the United States Government. Neither the United States Government nor any agency thereof, nor any of their employees, makes any warranty, express or implied, or assumes any legal liability or responsibility for the accuracy, completeness, or usefulness of any information, apparatus, product, or process disclosed, or represents that its use would not infringe privately owned rights. Reference herein to any specific commercial product, process, or service by trade name, trademark, manufacturer, or otherwise does not necessarily constitute or imply its endorsement, recommendation, or favoring by the United States Government or any agency thereof. The views and opinions of authors expressed herein do not necessarily state or reflect those of the United States Government or any agency thereof.